Linking Geostatistical Methods: Co-Kriging – Principal Component Analysis (PCA); with Integrated Well Data and Seismic Cross Sections for Improved Hydrocarbon Prospecting (Case Study: Field X)

Ryan Bobby Andika[1] and Haritsari Dewi[1]*

[1]Department of Geophysical Engineering, Faculty of Mining and Petroleum Engineering, Institut Teknologi Bandung, Jalan Ganeca 10, Bandung 40132, Indonesia

**corresponding author email: ryanbobbyandikaandika@yahoo.com*

Abstract

In this era of globalization, the demand for energy is rising in tandem with social and economic development throughout the world. Current hydrocarbon demand is much greater than domestic crude oil and natural gas production. In order to bridge the gap between energy supply and demand, it is imperative to accelerate exploration activities and develop new effective and efficient techniques for discovering hydrocarbons. Therefore, this study presents a new method for integrating seismic inversion data and well data using geostatistical principles that allow for the high level of processing and interpretation expected nowadays. The main part of this paper will concern the preparation and processing of the input data, with the aim of constructing a map of hydrocarbon-potency distribution in a certain horizon. It will make use of principal component analysis (PCA) and the co-kriging method. In the case study of Field X, we analyze a single new dataset by applying PCA to every existing well that contains multivariate rock-physics data. The interpretation that can be extracted from the output gives us information about the hydrocarbon presence in a particular depth range. We use that output as our primary dataset from which our research map is constructed by applying the co-kriging method. We also rely on an acoustic impedance dataset that is available for a certain horizon to fulfill the co-kriging interpolation requirement. All of the acoustic impedance data and output data that result from the application of PCA in a particular horizon give strong correlation factors. Our resulting final map is also validated with information from proven hydrocarbon discoveries. It is demonstrated that the map gives accurate information suggesting the location of hydrocarbon potency, which will need some detailed follow-up work to enhance the distribution probabilities. This method can be considered for hydrocarbon prediction in any area of sparse well control.

Index Terms: co-kriging, PCA, spatial relations, well data, AI seismic inversion

1. Introduction

In earth sciences, we seldom have sufficient data to accurately reveal the entire underlying subsurface conditions. Typically, in prospecting hydrocarbon zonation, we have to estimate the input parameters for the entire area from only a few data points. The existence of log data from the wells facilitates the descriptions of the petrophysical rock parameters. The more well data, the more accurate the geological modelling will be, and the easier the lateral seismic interpretation will become. It is hoped that the distribution of petrophysical rock parameters can be estimated in any area of sparse well control, with seismic data as a guide. Therefore, spatial modelling techniques should be used to generate the best geological interpretation and understand the associated uncertainties.

Seismic inversion aims to reconstruct a quantitative model of the Earth's subsurface, by solving an inverse problem based on seismic measurements.[6] Seismic inversion can provide information about the physical properties of the

reservoir rocks and identify the layers of subsurface rocks through the acoustic impedance profile (AI). The value of the acoustic impedance obtained in the inversion process is its value at certain points, whereas what is required is the overall value in the area of interest. We must therefore use a technique to estimate the values in the vertical and lateral directions, and the methods used for this will be geostatistical.

Geostatistical methods are easily useable at low cost, and provide an adequate framework for incorporating exhaustive secondary information (AI seismic inversion data) to improve the estimates of the primary variables (generated from PCA). The present paper makes use of collocated co-kriging to incorporate AI seismic inversion data as secondary information for mapping the values of the petrophysical rock parameters obtained from the application of PCA to well data.

2. Materials and Methods

In this study, we split the data processing into two main steps: (i) preparation of the primary data by applying principal component analysis (PCA) to our well data set (log), and (ii) using collocated co-kriging to interpolate that primary data. The aim of the study is to create a distribution map of the hydrocarbon potency by making use of principal component score data, and a seismic inversion "acoustic impedance" horizon map as a secondary data set to apply collocated co-kriging. We use the programs Paradigm 14.0 and Xlstat to help in this research, especially for constructing the map and performing the PCA. A flowchart of the process is shown in ***Figure 1***.

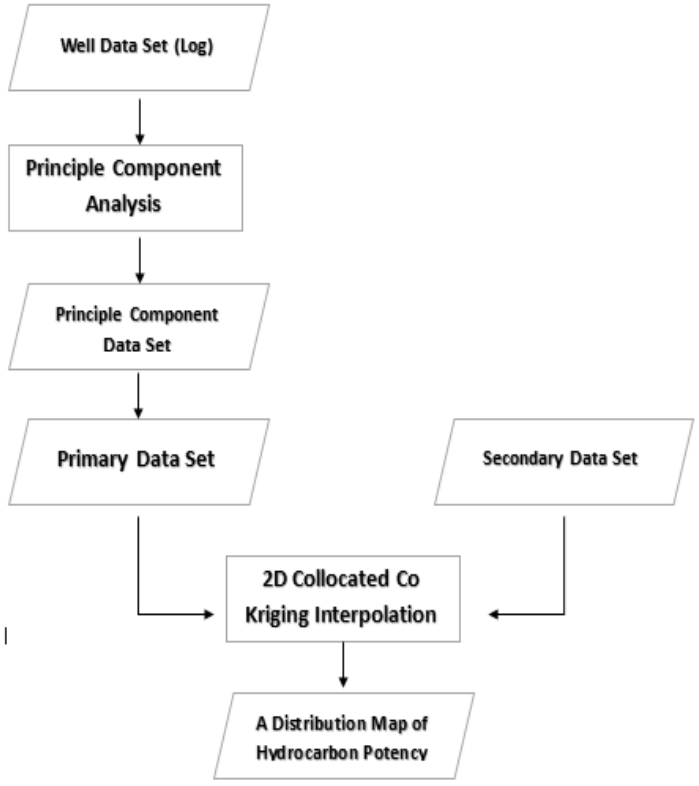

Figure 1. Flow diagram of the process.

2.1 Well data and principal component analysis

The physical data that has been compiled from each well is the main source of input data for the principal component analysis (PCA). Principal component analysis (PCA) is a multivariate data dimensionality reduction technique, used to simplify a data set to a smaller number of factors which explain most of the variability (variance).[1]

In this study, there are data from 5 well sites that have deviated mechanisms (i.e., the well is not drilled straight down) with different orientations. The physical characteristics that are used as input values for the PCA are ; GR (Iγ) – total gamma ray intensity [API], RLLD (ρLLD) – dual laterolog deep resistivity [Ω·m], NPHI (ΦN) – compensated neutron porosity [V/V], DEN (δ) – compensated bulk density [g/cm^3], and DT (Δt) – compensated sonic transit time [μs/ft].

The depth of the wells is about 1600 meters down from the subsurface. In actual fact, the distribution of well sites in the data acquired by PT Pertamina EP Asset 3 is clustered around the center of the low Acoustic Impedance (AI)-value map. There are four well sites that have been drilled in a specific alignment or orientation with 5-10 meter of spacing between each of them in the center of the AI Map, and one well site on the upper right side (outside the center of the AI map).

The first step toward generating the primary data from the principal component analysis is to produce a correlation matrix between each pair of variables using all the data from the wells in Field X, which we will label X-1, X-2, X-3, X-4, and X-5. Each well that we are using for prospecting has available data logs for five variables (NPHI, DT, RHOB, GR, and ILD). The matrix of correlations for the data from all the wells in Field X is shown in ***Tables 1 - 5***.

Table 1. Correlation matrix for well X-1

Variables	DT	GR	ILD	NPHI	RHOB
DT	1	0.338	-0.076	0.853	-0.653
GR	0.338	1	-0.063	0.291	0.024
ILD	-0.076	-0.063	1	-0.110	0.026
NPHI	0.853	0.291	-0.110	1	-0.785
RHOB	-0.653	0.024	0.026	-0.785	1

Table 2. Correlation matrix for well X-2

Variables	DT	GR	ILD	NPHI	RHOB
DT	1	0.251	-0.064	0.016	-0.196
GR	0.251	1	-0.106	0.013	0.466
ILD	-0.064	-0.106	1	-0.001	0.035
NPHI	0.016	0.13	-0.001	1	-0.004
RHOB	-0/196	0.466	0.035	-0.004	1

Table 3. Correlation matrix for well X-3

Variables	DT	GR	ILD	NPHI	RHOB
DT	1	0.288	-0.040	0.586	-0.250
GR	0.288	1	-0.065	0.601	0.509
ILD	-0.040	-0.065	1	-0.098	-0.041
NPHI	0.586	0.601	-0.098	1	-0.183
RHOB	-0.250	0.509	-0.041	-0.183	1

Table 4. Correlation matrix for well X-4

Variables	DT	GR	ILD	NPHI	RHOB
DT	1	0.635	-0.040	0.416	-0.250
GR	0.635	1	-0.065	0.646	0.509
ILD	0.416	0.646	1	-0.098	-0.041
NPHI	-0.198	-0.133	-0.098	1	-0.183
RHOB	0.142	0137	-0.041	-0.558	1

Table 5. Correlation matrix for well X-5

Variables	DT	GR	ILD	NPHI	RHOB
DT	1	0.739	-0.138	0.776	-0.366
GR	0.739	1	-0.195	0.773	-0.016
ILD	-0.138	-0.195	1	-0.145	-0.155
NPHI	0.776	0.773	-0.145	1	-0.535
RHOB	-0.366	-0.016	-0.155	-0.535	1

From the correlation matrices, we have extracted the eigenvalues for each of the wells as a second step in performing the PCA. These eigenvalues determine the principal components for each dataset, and more importantly the share of the variance due to each component. In this study, the PCA of the well data for Field X produces 5 separate principal components. The eigenvalues for each of the observed fields are shown in ***Tables 6 - 10***.

Table 6. Eigenvalues for well X-1

	F1	F2	F3	F4	F5
Eigenvalue	2.623	1.057	0.957	0.255	0.109
Variability	52.450	21.134	19.144	5.096	2.176
Cumulative	52.450	73.584	92.728	97.824	100.000

Table 7. Eigenvalues for well X-2

	F1	F2	F3	F4	F5
Eigenvalue	1.478	1.202	1.000	0.952	0.368
Variability	29.569	24.036	19.997	19.043	7.354
Cumulative	29.569	53.605	73.603	92.646	100.000

Table 8. Eigenvalues for well X-3

	F1	F2	F3	F4	F5
Eigenvalue	2.011	1.448	0.985	0.441	0.116
Variability	40.220	28.957	19.693	8.816	2.313
Cumulative	40.220	69.177	88.870	97.687	100.000

Table 9. Eigenvalues for well X-4

	F1	F2	F3	F4	F5
Eigenvalue	2.238	1.366	0.926	0.395	0.076
Variability	44.757	27.319	18.514	7.896	1.514
Cumulative	44.757	72.077	90.590	98.486	100.000

Table 10. Eigenvalues for well X-5

	F1	F2	F3	F4	F5
Eigenvalue	2.725	1.217	0.756	0.241	0.062
Variability	54.497	24.344	15.115	4.812	1.232
Cumulative	54.497	78.841	93.956	98.768	100.000

The eigenvalues for each set of well data yield the corresponding eigenvectors and factor loadings, which will shortly be used to construct the new projected data set. The eigenvalues are determined by **Equation 1**.

$$AV_1 = \lambda V_1 \quad (1)$$

Here, A is any of the correlation matrices, λ is an eigenvalue, and V_1 is the corresponding eigenvector. The eigenvalues and loading factors for each well are shown in ***Tables 11 - 15***.

Table 11. Eigenvectors for well X-1

	F1	F2	F3	F4	F5
DT	0.570	0.026	0.081	0.683	-0.449
GR	0.221	0.722	0.550	-0.342	-0.099
ILD	-0.084	-0.575	0.812	0.024	0.043
NPHI	0.595	-0.046	-0.014	0.034	0.802
RHOB	-0.515	0.380	0.177	0.644	0.380

Table 12. Eigenvectors for well X-2

	F1	F2	F3	F4	F5
DT	0.138	0.775	0.004	0.433	-0.438
GR	0.735	-0.167	-0.003	0.119	0.646
ILD	-0.133	-0.412	0.187	0.876	0.098
NPHI	0.018	0.082	0.982	-0.168	-0.006
RHOB	0.650	-0.441	0.013	-0.043	-0.617

Table 13. Eigenvectors for well X-3

	F1	F2	F3	F4	F5
DT	0.521	-0.360	0.060	-0.771	0.020
GR	0.555	0.456	0.119	0.188	0.659
ILD	-0.119	-0.071	0.989	0.028	-0.037
NPHI	0.636	-0.166	0.030	0.495	-0.567
RHOB	0.040	0.793	0.053	-0.352	-0.492

Table 14. Eigenvectors for well X-4

	F1	F2	F3	F4	F5
DT	0.507	0.367	-0.001	0.780	-0.006
GR	0.570	0.289	0.191	-0.511	-0.542
ILD	0.577	-0.351	0.195	-0.205	0.68
NPHI	-0.245	0.088	0.958	0.119	0.015
RHOB	-0.157	0.807	-0.088	-0.274	0.491

Table 15. Eigenvectors for well X-5

	F1	F2	F3	F4	F5
DT	0.551	-0.011	0.112	0.821	0.097
GR	0.512	-0.294	0.416	-0.332	-0.606
ILD	-0.125	0.685	0.715	-0.012	0.061
NPHI	0.578	0.086	-0.046	-0.460	0.667
RHOB	-0.290	-0.661	0.548	0.062	0.418

Table 16. Factor loadings for well X-1

	F1	F2	F3	F4	F5
DT	0.923	0.027	0.080	0.345	-0.148
GR	0.358	0.743	0.538	-0.173	-0.033
ILD	-0.084	-0.575	0.812	0.024	0.014
NPHI	0.595	-0.046	-0.014	0.034	0.264
RHOB	-0.515	0.380	0.177	0.644	0.125

Table 17. Factor loadings for well X-2

	F1	F2	F3	F4	F5
DT	0.168	0.850	0.004	0.423	-0.266
GR	0.894	0.183	-0.003	0.116	0.392
ILD	-0.162	-0.452	0.187	0.855	0.059
NPHI	0.022	0.089	0.982	-0.164	-0.004
RHOB	0.790	-0.484	0.013	-0.042	-0.374

Table 18. Factor loadings for well X-3

	F1	F2	F3	F4	F5
DT	0.739	-0.433	0.059	-0.529	0.007
GR	0.787	0.549	0.118	0.125	0.224
ILD	-0.169	-0.085	0.982	0.018	-0.013
NPHI	0.902	-0.200	0.030	0.329	-0.193
RHOB	0.057	0.955	0.053	-0.234	-0.167

Table 19. Factor loadings for well X-4

	F1	F2	F3	F4	F5
DT	0.759	0.429	-0.001	0.490	-0.002
GR	0.853	0.337	0.184	-0.321	-0.149
ILD	-0.366	0.103	0.922	0.075	0.004
NPHI	0.863	-0.410	0.187	-0.129	0.187
RHOB	-0.235	0.943	-0.084	-0.172	0.135

Table 20. Factor loadings for well X-5

	F1	F2	F3	F4	F5
DT	0.910	-0.012	0.097	0.403	0.024
GR	0.845	-0.324	0.362	-0.163	-0.150
ILD	-0.206	0.755	0.622	-0.006	0.015
NPHI	0.954	0.095	-0.040	-0.226	0.165
RHOB	-0.479	-0.730	0.476	0.030	0.104

The transformation of the primary data into a projected data set by making use of the information about the components is a critical step in PCA. The multivariate information carried by the primary data acts as input data for the next step in the process. This multivariate information will provide fundamental guidance for the interpretation of the interpolated data map that will result from the collocated co-kriging.

In this study, we will choose a principal component that has a high loading factor for the variables GR, NPHI, and DT. For this reason, we stipulate that for wells X-1, X-3, X-4, and X-5 we will be using Component 1 (F1) and for well X-2 Component 2 (F2). The purpose of this selection is to allow us to interpolate the primary data while retaining information about the porous rock stratum and the hydrocarbon (gas or oil) potency.

After calculating the eigenvectors for each set of well data and selecting single components, the next step is to construct a new data set called the principal component scores (PCS). It should be noted that the PCS is a projected data set that carries information about the primary data and is built from the factor loadings. The values of the PCS for each well are shown in ***Tables 21 – 25***.

Table 21. Principal component scores for well X-1

Observation	F1	F2	F3	F4	F5	DEPTH
Obs1	2.54	-0.269	-0.103	0.339	1.302	974.286
Obs2	2.38	-0.27	-0.123	0.135	1.532	974.438
Obs3	2.24	-0.30	-0.156	-0.048	1.586	974.59
Obs4	2.26	-0.46	-0.467	-0.244	-0.356	974.743
…	…	…	…	…	…	…

Table 22. Principal component scores for well X-2

Observation	F1	F2	F3	F4	F5	DEPTH
Obs1	1.871	0.138	0.046	0.445	-2.379	1122.115
Obs2	0.467	1.669	0.018	0.789	-0.960	1122.267
Obs3	0.390	1.921	0.018	0.874	-0.785	1122.42
Obs4	0.285	2.399	0.013	1.085	-0.722	1122.572
…	…	…	…	…	…	…

Table 23. Principal component scores for well X-3

Observation	F1	F2	F3	F4	F5	DEPTH
Obs1	3.659	-3.914	0.246	-5.055	-0.065	1148.012
Obs2	3.456	-4.394	0.236	-5.695	0.344	1148.165
Obs3	3.574	-2.751	0.412	-6.916	-0.605	1148.317
Obs4	3.575	-2.437	0.523	-7.292	-0.678	1148.47
…	…	…	…	…	…	…

Table 24. Principal component scores for well X-4

Observation	F1	F2	F3	F4	F5	DEPTH
Obs1	-2.069	-1.728	-0.748	0.325	-0.439	1533.144
Obs2	-2.065	-1.833	-0.732	0.281	-0.443	1533.296
Obs3	-2.241	-2.114	-0.706	-0.092	-0.326	1533.449
Obs4	-2.139	-2.232	-0.670	-0.094	-0.298	1533.601
…	…	…	…	…	…	…

Table 25. Principal component scores for well X-5

Observation	F1	F2	F3	F4	F5	DEPTH
Obs1	1.425	3.082	-3.025	-2.855	-0.427	1593.189
Obs2	1.589	2.989	-2.884	-2.428	0.146	1593.342
Obs3	1.331	2.847	-2.718	-2.291	0.331	1593.494
Obs4	0.948	2.889	-2.775	-2.524	-0.480	1593.647
…	…	…	…	…	…	…

The conditioning step for the primary data is now complete.

2.2 Acoustic impedance map and collocated co-kriging

In this study, we use the map of the acoustic impedances of the Z-14 horizons in Field X, which provides an indication of the potential presence of hydrocarbon fluids. This field is located in the West Java Basin, in the Cibulakan Atas formation, which consists of a combination of shale, sandstone, and limestone (see ***Figure 2***).

The AI map that we make use of, as a secondary data set when applying the process of collocated co-kriging, has a spatial extent of 1440 x 2750 m^2. Collocated co-kriging is a variant of full co-kriging, where secondary data used for estimation are reduced so as to retain only the secondary datum in the location where the primary variable is being estimated.[4,7] The Z-14 horizon is located at around 1600 m depth, with a variable AI score ranging from 7000 rayl to 10,000 rayl in each sector of the map (as can be seen in the color bar of the AI map in ***Figure 4***). The inversion AI data for the Z-14 horizon of Field X that we use to perform the collocated co-kriging is the property of PT Pertamina EP Asset 3. It was produced by model-based inversion theory (see ***Figure 3***).

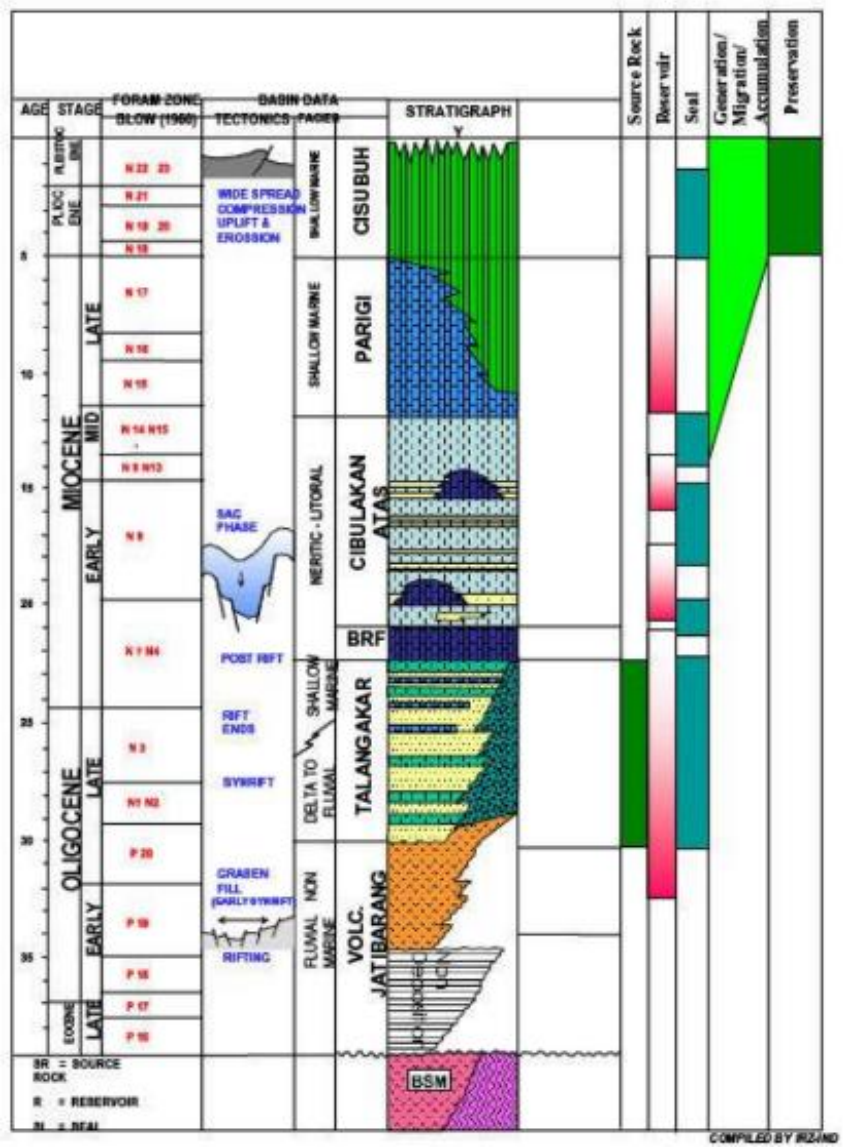

Figure 2. Stratigraphy of West Java Basin[2]

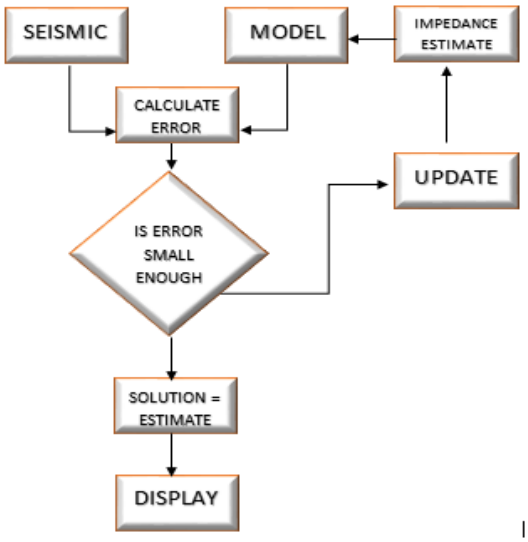

Figure 3. Flow diagram of model-based inversion method

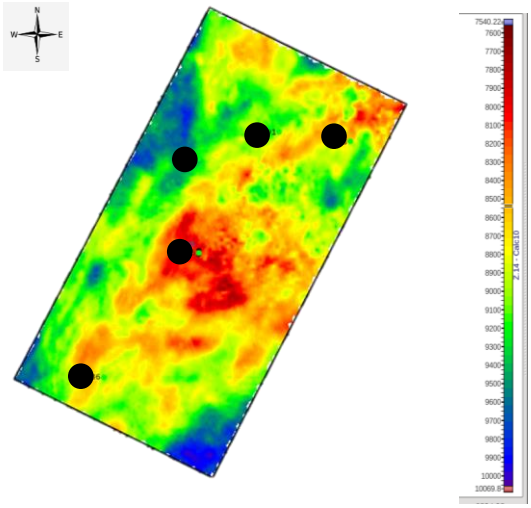

Figure 4. Map of the acoustic impedance with the distribution of PCS for the primary data (black dots)

Based on the given information about the acoustic impedance of the Z-14 horizon, it is clear that there is a low value of the acoustic impedance in the center and upper right of the map. The variable scores can be interpreted as being due to the presence of a porous (not compacted) rock stratum in Field X that contains fluids. This particular data set is one of the considerations that led PT Pertamina EP Asset 3 to decide to make some delineations and collect well log data at several locations, as there was a high probability of a hydrocarbon prospect there.

As mentioned above, the intention is to apply collocated co-kriging to interpolate the values of the PCS extracted from the well log data. Remembering that the well sites deviate from the vertical with different orientations, the intersections of the wells and the Z-14 horizon have different depths on the AI map. So in this case, the PCS at the intersections between the wells and the Z-14 Horizon (at the depth of the horizon) are taken as input data (see ***Figure 5*** and ***Table 26***).

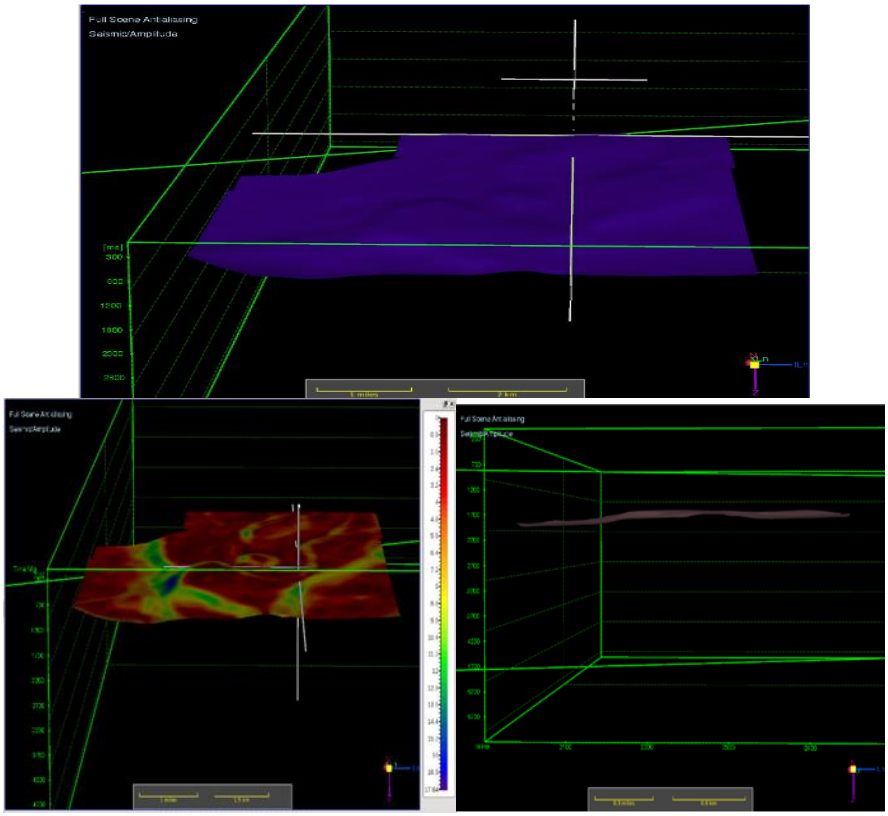

Figure 5. The horizon map of Field X

Table 26. The Primary Data Input from the PCS

No Well	Depth	PC Score
X-1	1669.31	3.921
X-2	1665.66	-0.22
X-3	1687.51	1.345
X-4	1696.2	1.301
X-5	1657.64	1.631

The data from the available results of the PCS are used as primary input, and the AI seismic inversion map as densely sampled secondary input data. In addition, to improve the interpolation accuracy, the correlation between the primary and secondary variables should be as high as possible. Therefore we must construct a cross plot between both sets of data.

The red dots in ***Figure 6*** correspond to data sampled from the primary and secondary variables, which have a correlation factor of about -0.765. The cross plot is used to measure the strength of the relationship between the two variables. A negative correlation means that as the value of one variable increases, the other decreases.

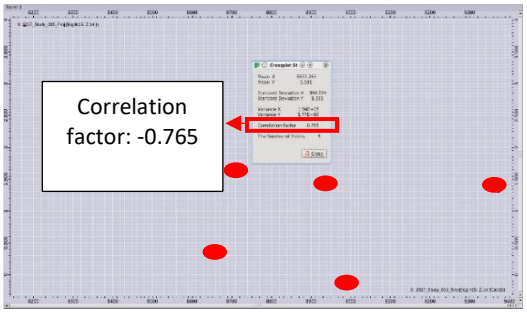

Figure 6. Correlation factor

Collocated co-kriging represents the spatial relationship of the control data in the form of a variogram such as ***Figure 7***. Two important criteria that show the consistency of the spatial structure are the range and the relative nugget effect (nugget effect/sill: *C*0/*C*). The variogram that is more appropriate has a greater range and smaller nugget effect. The variogram below has no nugget effect, with a range of 1218.28 and a sill of 2.53.

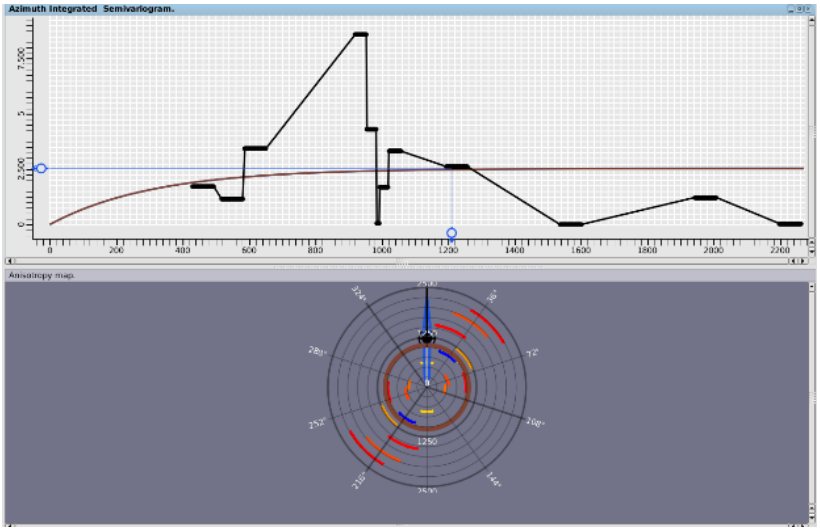

Figure 7. Collocated co-kriging variogram

3. Results

Based on the processed output data from Field X, there is a significant hydrocarbon potency in the field, but not at every spot that wasn't sampled. The magnitude of the hydrocarbon potency at each interpolated spot can be examined quantitatively using the color-bar of the map in ***Figure 8***.

The red color intervals are in the range 2.8-3.5 (dimensionless), which can be considered as areas of potential hydrocarbon content having high PCS values. All of the interpolated data, as stated before, refers to the primary data, reduced to principal component Scores (PCS) which contain "multivariate (many variables) information". The variables that contribute to this particular PCS, in this study, are NPHI, GR, and DT. These three variables coherently give information about the presence, or not, of hydrocarbon fluid content and tend to indicate porosity.[3]

The Wyllie formula for calculating sonic porosity can be used to determine porosity in consolidated sandstones and carbonates with intergranular porosity (grainstone) or intercrystalline porosity (sucroise dolomites).[2] Meanwhile, NPHI can be used to calculate vuggy or fracture secondary porosity in carbonates by comparing it to the total porosity. The fracture secondary porosity is found by subtracting the sonic porosity from the total porosity. The Wyllie equation reads:

$$\emptyset_{sonic} = \left(\frac{\Delta t_{log} - \Delta t_{ma}}{\Delta t_f - \Delta t_{ma}}\right) \times 1/Cp \qquad (2)$$

where

$\emptyset_{sonic}$ = sonic derived porosity
Δt_{ma} = interval transit time of the matrix
Δt_{log} = interval transit time of formation
Δt_f = interval transit time of the fluid in the well bore
(fresh mud = 189; salt mud = 185)
Cp = compaction factor

The compaction factor can be calculated from the formula:

$$Cp = \frac{\Delta t_{sh} \times C}{100} \qquad (3)$$

where

Δt_{sh} = interval transit time for adjacent shale
C = a constant which is normally[5] 1.0

It can clearly be seen that the high PCS are in general located in the center, left, and lower right corner of the map in ***Figure 8***. These results are completely different from the hydrocarbon potency for Field X predicted from the quantitative values of the acoustic impedance.

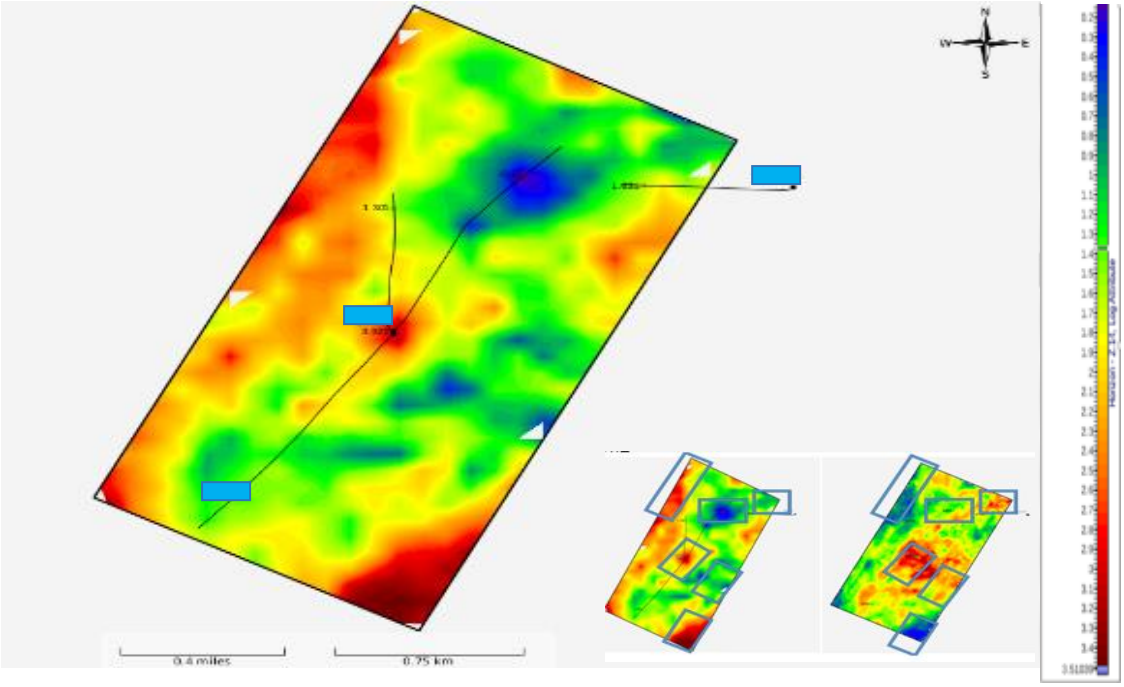

Figure 8. A distribution map of the hydrocarbon potency generated by collocated co-kriging

4. Discussion and Conclusion

Here we identify six different zones in the potency map generated by our analysis, which would need some detailed exploration to reveal the accuracy of our hydrocarbon prospecting. It can be positively stated that low values of the AI (red color) for the Z-14 horizon of Field X, should not be regarded as an infallible indicator of hydrocarbon potency in all cases. Our study is based on the application of collocated co-kriging to interpolate the PCS data from all the wells in Field X. Our study simply adds extra information to what is already known about the potency of hydrocarbon discovery at the site, building the AI score, and the interpolated PCS map can be worthwhile as a controlling or enhancing factor if and when it is decided to drill further prospect delineation wells.

In this study, we have performed a quantitative and qualitative test to determine whether the PCS interpolated map is scientifically and intuitively adequate for hydrocarbon prospecting. The quantitative test that we came up was to construct a "cross-plot" section between the primary and secondary data, as shown in ***Figure 6***. The cross-plot in this case has a correlation factor about -0.765 which is close to -1. This indicates a strong relationship between the two data sets. Moreover, the fact that the correlation factor is negative, in this case, signals a reverse relationship between the PCS and the AI seismic inversion data.

Now that the PCS have been interpolated by collocated co-kriging, we continue our interpretation by examining well X-1, which is located at the center of our output map in ***Figure 9.*** This well intersects the Z-14 horizon in the red colored zone on the output map. We also have data from Pertamina EP Asset 3 that gives us information about the gas production from this well (see ***Figure 10***). This information allows us to extend our predictions to gas potency in the area, which is highest in the red colored zones in an output map very similar to ***Figure 9.*** Even though we are predicting that most of the red-colored zones have high gas potency, we are not recommending HD3 because that zone is located relatively far from all the sampled wells.

What about the blue colored zones in ***Figure 9***? We can also make some predictions for those zones. As a starting point for these predictions, we use the production performance data we have for well X-2. In this well, the production is dominated by oil

(see ***Figure 11***). In view of this, we have identified 5 blue zones in ***Figure 12*** that we expect to have high oil potency, although more detailed exploration would be needed to test the accuracy of this hydrocarbon prospecting**.**

We can also perform a qualitative validation of the accuracy of the combined PCA and collocated co-kriging results by estimating the hydrocarbon potency in an un-sampled area. As we stated before, all the well data and the acoustic impedance map used in this study are the property of PT Pertamina EP Asset 3. The total data set from Field X includes data from a sixth well. We can therefore perform a validation of the PCS map generated in this study by using all the well data for Field X. We have used the data from the first five well (X-1, X-2, X-3, X-4, and X-5) to predict the hydrocarbon potency in Field X, and the validation data comes from the sixth well (X-6). The validation data from X-6 is shown in the production performance graph for the Z-14 horizon in ***Figure 13***.

Based on the wells location data we have for the Z-14 Horizon, well X-6 is located in zone HD1 (see ***Figure 9*)**. In any case, a comprehensive further geological and geophysics analysis is needed for zones HD2, HD3, HD4, and RBA1-RBA5 to check the potential presence of hydrocarbons.

Moreover, it can be concluded that the PCS distribution map generated from the combined PCA-collocated co-kriging method has successfully mapped the hydrocarbon potency as a guide for more detailed exploration in Field X.

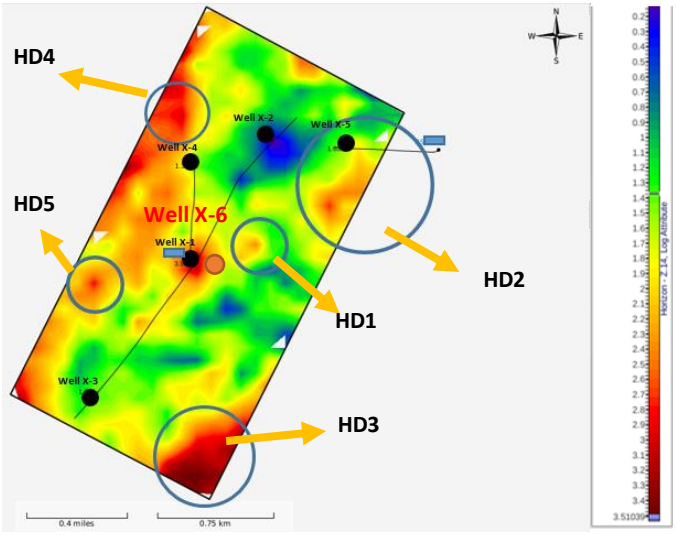

Figure 9. Six different zones in the distribution map with high hydrocarbon potency generated by the collocated co-kriging and the acoustic impedance map

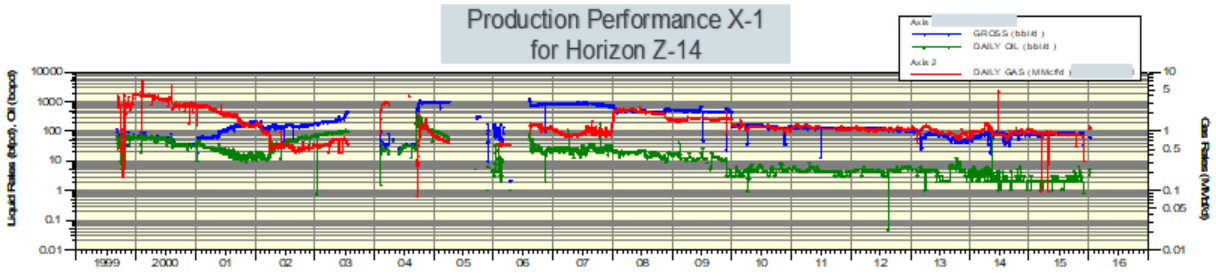

Figure 10. Production performance for Well X-1

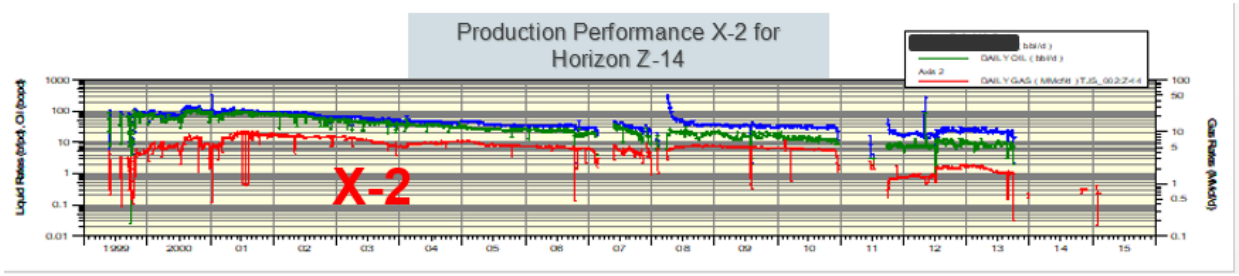

Figure 11. Production performance for Well X-2

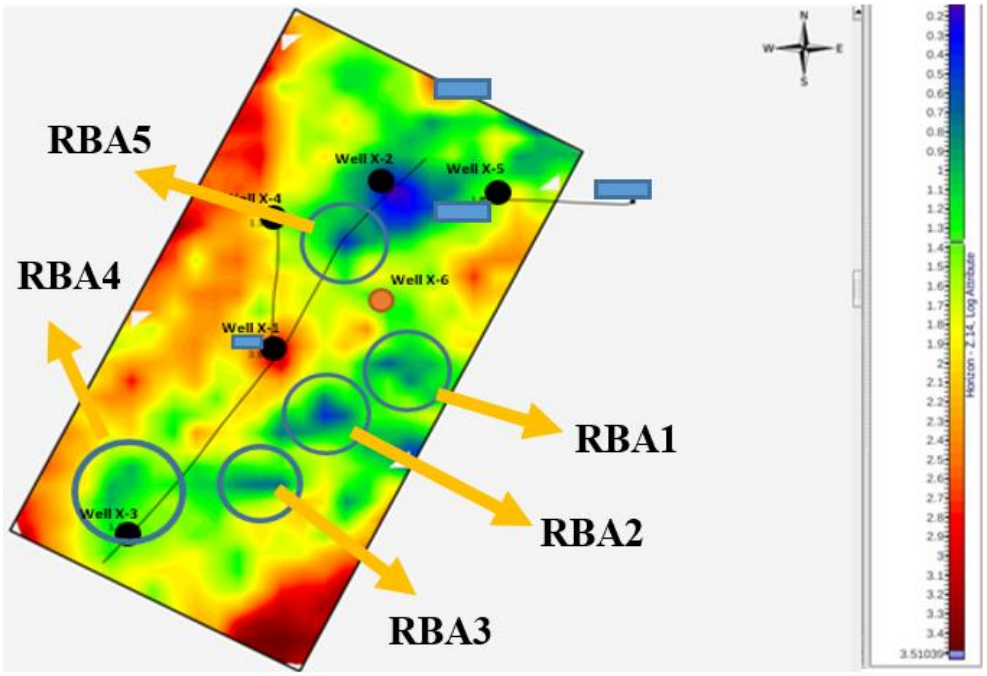

Figure 12. Blue colored zones predicted to have high oil potency

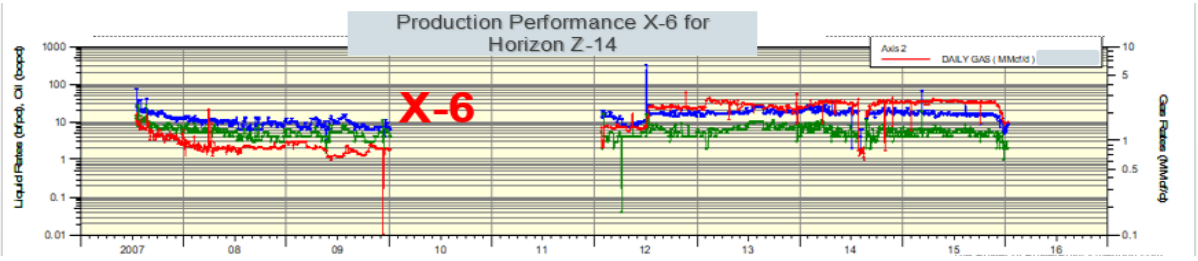

Figure 13. Production performance of well X-6 (upper) for the Z-14 horizon.

Acknowledgements

We would like to extend our sincere gratitude to PT Pertamina EP Asset 3, especially to Mr Dias Pramudito and Mr Andreas Wasi for their help and support in using their data and software. Thanks also to our beloved lecturer, Ms Susasnti Alawiyah in Bandung Institute of Technology for her assistance, guidance and support in all phases of this study.

References

[1] G. Andrei and B. M. Niculescu, "Principal component analysis as a tool for enhanced well log interpretation", *Geoscience 2016*.

[2] D. Arpandi and S. Patmokismo, "The Cibulakan Formation as one of the most prospective stratigraphic units in the north-west Java basinal area", *IPA Proceedings*, **1975**, 181-210.

[3] G. Asquith and C. Gibson, *Basic Well Log Analysis for Geologists: Methods in Exloration Series*, American Association of Petroleum Geologists, **1982**, Tulsa, Oklahoma.

[4] M. N. M. Boezio, J. F. C. L. Costa and J. C. Koppe, "Kriging with an external drift versus collocated co-kriging for water table mapping", *Applied Earth Science*, **2006**, 115(3), 103-112.

[5] D. W. Hilchie, *Applied Openhole Log Interpretation for Geologists and Petroleum Engineers*, Colorado School of Mines, **1978**.

[6] Y. Wang, *Seismic Inversion: Theory and Applications*, **2016**, John Wiley and Sons.

[7] W. Xu, T. Tran, R. M. Srivastava, and A. G. Journel, "Integrating seismic data in reservoir modelling: the collocated co-kriging alternative", *SPE annual technical conference and exhibition*, **1992**, Society of Petroleum Engineers.